Research Article

Robust Hybrid Controller Design to Stabilise an Underactuated Robot Vehicle under Various Input

Yomna Sabah Hussein [ID],[1] **Haider Galil Kamil,**[1,2] **and Ahmed Abdulhadi Al-Moadhen** [ID][1]

[1]*Department of Electrical & Electronic Engineering, College of Engineering, University of Kerbala, Kerbala, Iraq*
[2]*Department of Computer Engineering Techniques, AlSafwa University College, Kerbala, Iraq*

Correspondence should be addressed to Yomna Sabah Hussein; yomna.s@s.uokerbala.edu.iq

This paper presents the design of the control system for a robot vehicle with two wheels that mimics a double Inverted Pendulum (IP) system with an extendable payload. By expanding the degrees of freedom, the system is more flexible. Still, this model posed challenges for control of parts of the system, including the proper balancing of the intermediate body and angular displacement of both wheels and lifting the payload to the demanded height. In this paper, a hybrid control system that incorporates more than one type of controller which combined proportional integral derivative (PID), proportional derivative (PD), and fuzzy logic control (FLC) these controllers are designed for stabilising the aforementioned system. The controller was validated by applying different input signals to the payload actuator to prove the control system's stability and analyse the system's behaviour. The simulation results were satisfactory for the hybrid control technique. The wheels successfully stabilised within 1.2682 s. Further, the first and second links stabilised at 9.5953 s and 9.6467 s, respectively. The payload approximately produces the same input signal applied to the payload actuator. The model was derived using the Euler–Lagrange equation. The equations are solved using kinetic energy and potential energy which employs for motion. Simulation results of the two-wheeled robot vehicle with extendable payload designed with hybrid control systems are implemented using MATLAB/Simulink environment.

1. Introduction

The proposed robot vehicle is based on a double IP which is considered a nonlinear and unstable system [1–3]. The IP system and its applications play a vital role in control system engineering and research because of its highly underactuated nature and complex strong-coupling system [3, 4]. In the subject of control engineering, IP problems are very common. Previous research studied the problem of stabilising IP and has reflected the development of many applications based on the same concept, including the design of a classical pendulum on a cart [5–7]. The IP systems have been extended and become more complicated with multiple rods which provides much flexibility [8], such as double IP [9–11] and triple IP [12–15]. Many pieces of research focused on applications based on IP systems, such as the Segway robot [16–18], the two wheelchairs [19–21], simple walking models [22], and the bipedal robot based on IP [23, 24].

Our research considered the five degrees of freedom model, consisting of two wheels and two links with a movable payload that can be moved to demand height. Increasing the system's degrees of freedom enables the vehicle to manoeuvre freely. Different input signals were applied to the movable payload to validate the system's stability. The wheels were assumed to move within 0.8 m while both links of the intermediate body of the system were retained as upright to ensure system stabilisation. The hybrid control system was used as a control technique to implement five loops of model control to achieve system stability.

This paper is organised as follows: "system description" which describes the two-wheeled robot vehicle with movable payload and the "mathematical modelling" section, which explains the derivation of the nonlinear differential equations utilized in the system simulation. The section "hybrid control design" obtained the control system used for the

system stabilisation. The "Results Discussion" section discussed the simulation results. Finally, the research is concluded in the "conclusions" section.

2. System Description

A diagram form illustration of the assumed model [25] is shown in Figure 1. The system consists of two wheels and an intermediate body comprised of two links connected to the payload that can move to the required height. The robot vehicle drives these wheels using two DC motors, with a further motor used to drive the second link. A single actuator in the middle of the second link of the intermediate body lifts the payload to the required height. The robot vehicle thus has five degrees of freedom (DOF).

   (i) The translational motion of the two wheels

   (ii) The two links of the system

   (iii) The movable payload linear actuator

The angles of both links, the first being θ_1 and the second θ_2, were measured from the **Z**-axis, representing the intermediate body being in the upright position or inclined to only a small degree, depending on the controller design. **Q** is the linear displacement of the payload measured from the $\mathbf{O_2}$ position along with the second link. The left $\delta_{\mathbf{L}}$ and right $\delta_{\mathbf{R}}$ wheels' angular displacements cause the vehicle to move linearly in the **XY** plane. These are the main five loops controlled to stabilise the system.

3. Mathematical Modelling

The system mathematical modelling was derived using the Euler–Lagrange equation due to modelling complex, nonlinearity, and strong-coupling systems such as [19, 26]. This method offers a simple approach to determining a complex systems model [18]. The Lagrange equation employs both kinetic energy and potential energy that are solved for motion [20, 27] using an equation as follows:

$$\frac{d}{dt}\left(\frac{\partial L}{\partial \dot{q}_i}\right) - \frac{\partial L}{\partial q_i} = Q_i. \tag{1}$$

After the system was derived it yields five nonlinear differential equations

$$
\begin{aligned}
&2C_{21}\ddot{\delta}_L + C_{22}\ddot{\delta}_R + C_9\frac{R_w}{2}L_1\ddot{\theta}_1\cos\theta_1 - C_9\frac{R_w}{2}L_1\dot{\theta}_1^2\sin\theta_1 + \frac{R_w}{2}\left(C_{10}+C_8Q\right)\ddot{\theta}_2\cos\theta_2 - \frac{R_w}{2}\left(C_{10}+C_8Q\right)\dot{\theta}_2^2\sin\theta_2 + \frac{R_w}{2}C_8\dot{Q}\dot{\theta}_2\cos\theta_2 \\
&= T_L - T_{fL}, 2C_{21}\ddot{\delta}_R + C_{22}\ddot{\delta}_L + C_9\frac{R_w}{2}L_1\ddot{\theta}_1\cos\theta_1 - C_9\frac{R_w}{2}L_1\dot{\theta}_1^2\sin\theta_1 + \frac{R_w}{2}\left(C_{10}+C_8Q\right)\ddot{\theta}_2\cos\theta_2 - \frac{R_w}{2}\left(C_{10}+C_8Q\right)\dot{\theta}_2^2\sin\theta_2 \\
&\quad + \frac{R_w}{2}C_8\dot{Q}\dot{\theta}_2\cos\theta_2 \\
&= T_R - T_{fR}, 2C_{18}\ddot{\theta}_1 + C_9\frac{R_w}{2}L_1\left(\ddot{\delta}_L+\ddot{\delta}_R\right)\cos\theta_1 - C_9\frac{R_w}{2}L_1\left(\dot{\delta}_L+\dot{\delta}_R\right)\dot{\theta}_1\sin\theta_1 + 2L_1\left(C_{10}+C_8Q\right)\ddot{\theta}_2\cos\left(\theta_1-\theta_2\right) \\
&\quad - 2L_1\left(C_{10}+C_8Q\right)\dot{\theta}_1\dot{\theta}_2\sin\left(\theta_1-\theta_2\right) + 2L_1\left(C_{10}+C_8Q\right)\dot{\theta}_2^2\sin\left(\theta_1-\theta_2\right) + 2L_1C_8\dot{Q}\dot{\theta}_2\cos\left(\theta_1-\theta_2\right) + C_9\frac{R_w}{2}L_1\dot{\theta}_1^2\left(\dot{\delta}_L+\dot{\delta}_R\right)\sin\theta_1 \\
&\quad + 2L_1\left(C_{10}+C_8Q\right)\dot{\theta}_1^2\dot{\theta}_2\sin\left(\theta_1-\theta_2\right) - C_3\,g\,\dot{\theta}_1\sin\theta_1 \\
&= 0.5\left(T_{LT}-T_{RT}\right), C_{20}\ddot{\theta}_2 + \left(C_{12}\dot{Q}+2C_8Q\right)\dot{\theta}_2 + \left(C_{12}Q+C_8Q^2\right)\ddot{\theta}_2 + \frac{R_w}{2}\left(C_{10}+C_8Q\right)\left(\ddot{\delta}_L+\ddot{\delta}_R\right)\cos\theta_2 \\
&\quad - \frac{R_w}{2}\left(C_{10}+C_8Q\right)\left(\dot{\delta}_L+\dot{\delta}_R\right)\dot{\theta}_2\sin\theta_2 + C_9\frac{R_w}{2}\dot{Q}\left(\dot{\delta}_L+\dot{\delta}_R\right)\cos\theta_2 + 2L_1\left(C_{10}+C_8Q\right)\ddot{\theta}_1\cos\left(\theta_1-\theta_2\right) \\
&\quad - 2L_1\left(C_{10}+C_8Q\right)\dot{\theta}_1^2\sin\left(\theta_1-\theta_2\right) + 2L_1\left(C_{10}+C_8Q\right)\dot{\theta}_1\dot{\theta}_2\sin\left(\theta_1-\theta_2\right) + 2C_8L_1\dot{\theta}_1\dot{\theta}_2\cos\left(\theta_1-\theta_2\right) \\
&\quad + \frac{R_w}{2}\left(C_{10}+C_8Q\right)\left(\dot{\delta}_L+\dot{\delta}_R\right)\dot{\theta}_2^2\sin\theta_2 - \left(C_{15}+C_8Q\right)g\dot{\theta}_2\sin\theta_2 - 2L_1\left(C_{10}+C_8Q\right)\dot{\theta}_1\dot{\theta}_2^2\sin\left(\theta_1-\theta_2\right) \\
&= T_{MT} - L_dF_d, C_8\ddot{Q} - \frac{1}{2}\left(C_{12}+2C_8Q\right)\dot{\theta}_2^2 - C_8\frac{R_w}{2}\dot{\theta}_2\left(\dot{\delta}_L+\dot{\delta}_R\right)\cos\theta_2 - 2L_1C_8\dot{\theta}_1\dot{\theta}_2\cos\left(\theta_1-\theta_2\right) + C_8g\cos\theta_2 = F_{aT}.
\end{aligned}
\tag{2}
$$

The system was built and the dynamics were described using these five nonlinear differential equations. The torques of the motors are the system's inputs including $T_{LT}T_{RT}$. The motor derived the second link T_{MT}, and the linear actuator force is F_{aT} where J_w, J_1, J_{2u}, J_{2l}, and J_m are the intermediate body's mass moment of inertia. The system simulation parameters reported by [28] that based on the standard dimensions of a two-wheeled robot vehicle illustrated in Table 1.

3.1. Hybrid Control Design. The hybrid control system intends to improve the system performance by combing the best specifications from the control systems used [29, 30]. A hybrid control system employs the beneficial sides of the proposed controllers suggested [31]. This study implements hybrid controllers to improve performance.

The first control system was the PID controller, a widely used control system that provides dependable and stable performance for most systems [32, 33]. The proposed
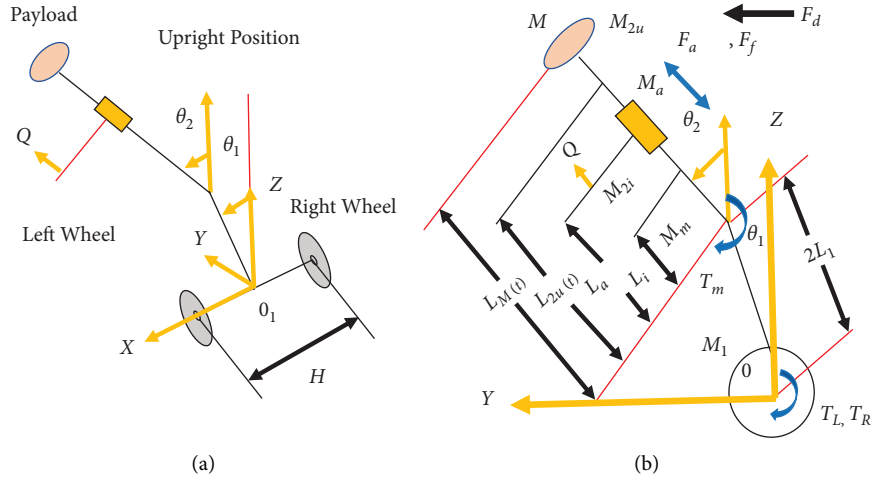
FIGURE 1: The main parts of the vehicle on two different sides.

TABLE 1: The parameters of a two-wheeled robot vehicle with a movable payload.

Variable	Value	Unit
M_m	0.3	Kg
J_w	0.225	$Kg \cdot m^2$
R_w	0.3	m
M_l	3	Kg
J_1	0.003025	$Kg \cdot m^2$
M_{2l}	1.5	Kg
M_{2u}	1.5	Kg
J_{2u}	0.005	$Kg \cdot m^2$
J_{2l}	0.005	$Kg \cdot m^2$
M	70	Kg
J_M	1	$Kg \cdot m^2$

controller is a commonly used control system because it is simple and easy to tune, further providing robust performance [34]. Then the fuzzy logic controllers test the system stability and the improvement of this type of controller on the system. In this research, higher control efforts were exerted in PID than in FLC for the system stabilisation. However, it is essential to decrease the exerted effort of the controller to stabilise the system. According to the simulation results, the FLC was significantly reduced compared to PID controllers by the control effort made for system stabilisation, without impacting the stability of the system. After that, the hybrid control system intends to improve the system performance by combing the good specifications from the PID and FLC control systems used [35].

Two types of hybrid control systems are designed for the nonlinear model for two-wheeled robot vehicles with movable payload. PID with FLC is used to control both wheels, two links of the intermediate body, while the payload actuator was controlled using PD with FLC controllers.

The PID-PD control parameters are tuned progressively until the system stabilise [36]. The FLC with two inputs includes error and change of error with one output used to describe a fuzzy inference system and then create the fuzzy rules [37, 38]. The linguistic variable of the two inputs and

output are negative-big (NB), negative-small (NS), zero (Z), positive-big (PB), and positive-small (PS). These rules yield the action of the FLC parts. The proper system tuning of the FLC to stabilise the model was developed using five Gaussian membership functions (MF) with 25 rules base. Figure 2 illustrated the design of the model with the hybrid control system.

For PID and PD tuning, the gain parameters are shown in Table 2.

The fuzzy logic control with 25 rules base and five MF are shown in Table 3 depending on the desired system performance.

The membership functions are illustrated in Figure 3.

4. Analysis and Discussion of Simulation Results

At this stage, the system was designed with different force input signals applied to the payload to validate the control system's robustness. A hybrid control system is designed to stabilise combined with PID-PD and FLC. The system responses were tested with various input signals applied to the payload actuator.

4.1. Test 1: Simulation Results with the First Payload Input Signal. The first input signal is illustrated in Figure 4. These simulation results of the system response using hybrid controllers are illustrated in Figure 5. The results clearly show that the control system stabilised the two wheels robot vehicle. The system controller effort is observed in Figure 6. It can be seen that the wheels stabilised with acceptable overshoot and peaks for the wheels, and the two links and a 4.954% overshoot were observed on the payload actuator.

Simulation results for the system response using hybrid controllers are illustrated in Figure 5.

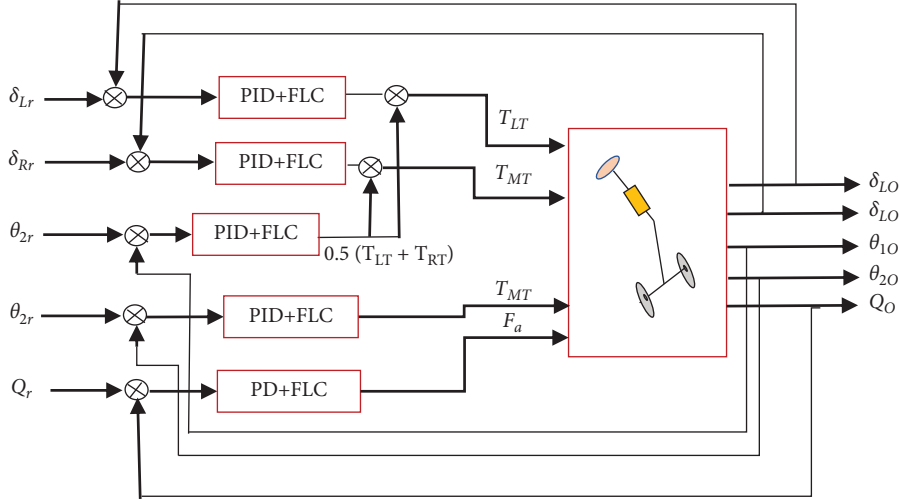The exerted effort of the controllers required to stabilise the system is represented in Figure 6.

FIGURE 2: The system block diagram using hybrid controllers.

TABLE 2: PID and PD gain parameters.

Loop	PID gains		
	Kp	Kd	Ki
Left wheel	50	1	0.01
Right wheel	50	1	0.01
First link	10	2	$0.1\,e^{-3}$
Second link	6	7	0.8
Payload actuator	20	10	0

TABLE 3: 25 fuzzy controller rules base.

$\dot{e}$	NB	NS	Z	PS	PB
NB	NB	NB	NB	NS	Z
NS	NB	NB	NS	Z	PS
Z	NB	NS	Z	PS	PB
PS	NS	Z	PS	PB	PB
PB	Z	PS	PB	PB	PB

The hybrid controller was able to help stabilise the system components with the controllers' effort as shown in Figure 6. The wheels settle at 1.2682 s with a 4.737% overshoot. The first link of the intermediate body reached settling time at 0.0621 s, and the second link settled at 4.529 s, and the payload actuator produce the same input signal applied to the payload with a 4.954% overshoot.

4.2. Test 2: Simulation Results with the Second Payload Input Signal. The second input signal using a hybrid controller applied on the payload actuator is illustrated in Figure 7.

Simulation results for the system response using hybrid controllers are illustrated in Figure 8.

The exerted effort of the controllers required to stabilise the system is represented in Figure 9.

The hybrid controller was capable to stabilise the system parts with the second input signal, and the control system

effort was less than the first signal. The payload actuator produced the same input signal applied to the payload with a 0.515% overshoot.

4.3. Test 3: Simulation Results with the Third Payload Input Signal. The third input signal using a hybrid controller applied on the payload actuator is shown in Figure 10 and the system response is illustrated in Figure 11 further Figure 12 represents the control system effort used to stabilise the system.

Simulation results for the system response using the hybrid controllers are illustrated in Figure 11.

The exerted effort of the controllers required to stabilise the system is represented in Figure 12.

The system successfully stabilised with the third input signal, but the payload actuator required higher control effort for the payload stability, this is due to the sharp shape of the input signal. When the signal reaches the maximum point, it suddenly goes back to zero, which makes the controller require higher effort for the payload stabilisation.

4.4. Test 4: Simulation Results with the Fourth Payload Input Signal. The last test was with the input signal illustrated in Figure 13. In this case, the control system successfully stabilised with controller effort exerted for stabilisation, as shown in Figure 14.

Simulation results for the system response using the hybrid controllers are illustrated in Figure 15.

The exerted effort of the controllers required to stabilise the system is represented in Figure 14.

The hybrid controller stabilised the system parts with the fourth input signal and acceptable controller effort; The payload actuator produced the same input signal applied to the payload with an overshoot of 59.718%.

Two-hybrid controllers are implemented, including PID with FLC and PD with FLC. The hybrid controllers combined the excellent characteristics of the PID-PD and FLC
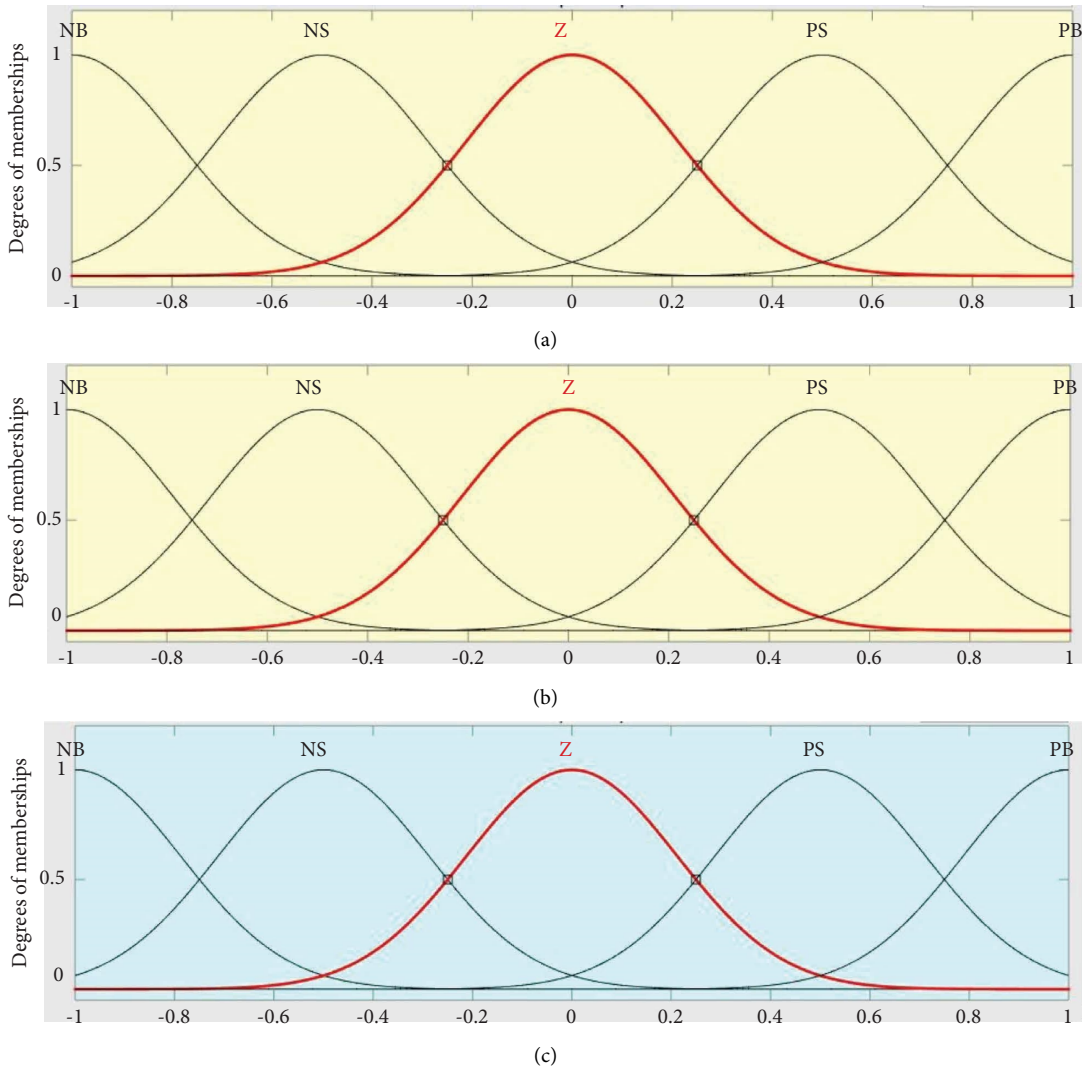
(a)

(b)

(c)

Figure 3: Gaussian membership function with two inputs and one output: (a) error, (b) change of error, and (c) output.
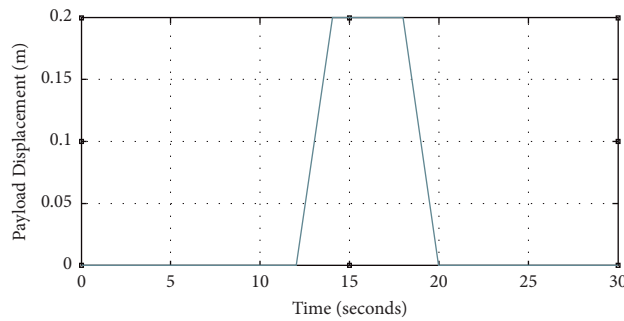

Figure 4: The first input signal applied on the payload.

control systems. The controllers successfully stabilised the model with different input signals applied on the payload linear actuator. These input signals validate the control system's stability, proving that the system is still stable with various input signals. The linear displacement for both wheels settled with 1.2682 s settling time and 4.737%

Left wheel displacement

Right wheel displacement

First link angle

Second link angle

Displacement of the payload
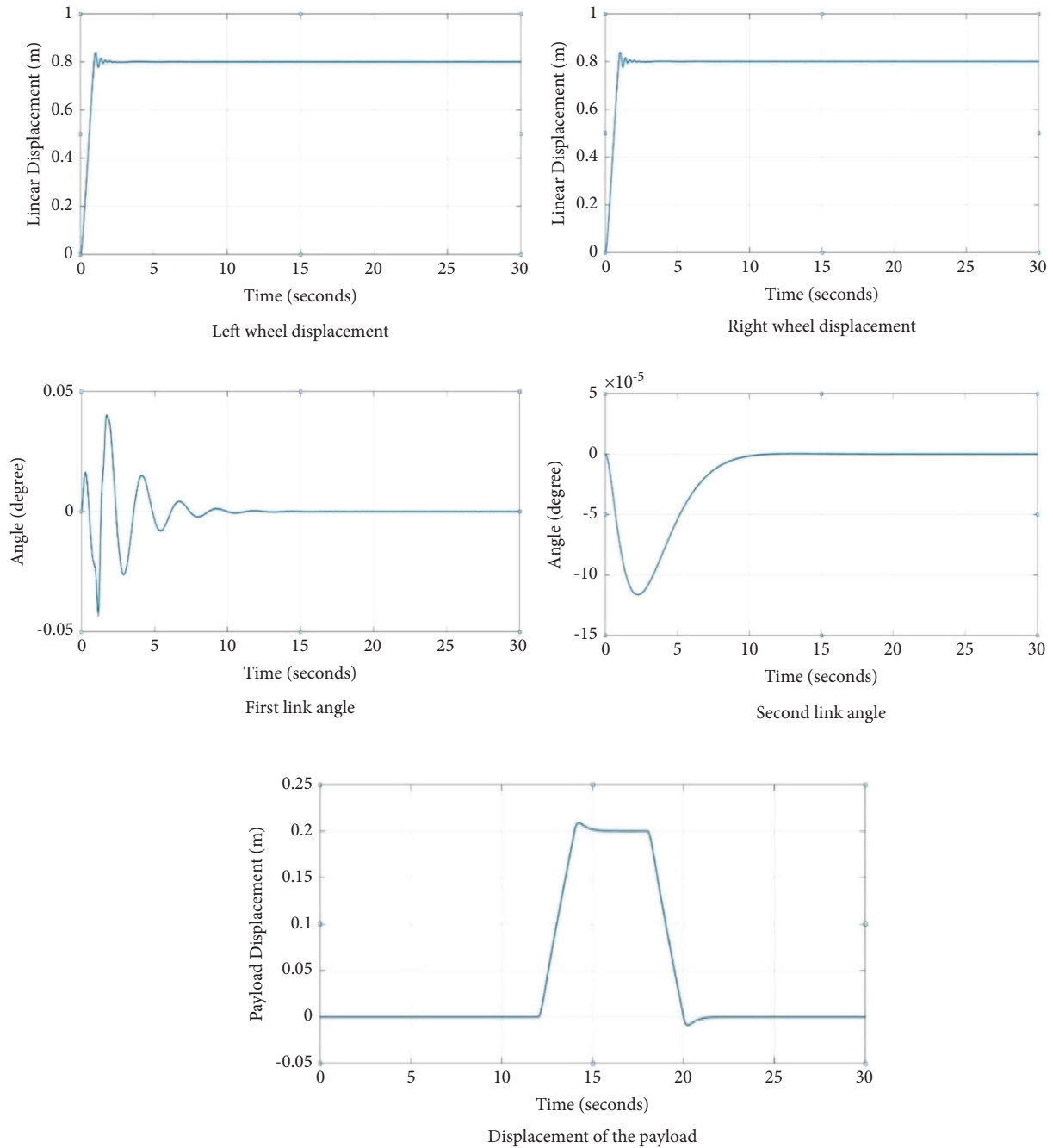
FIGURE 5: System response with the first input signal.

overshoot. The two links of the intermediate body successfully stabilised at the upright position. The first link settled at 9.5953 s, while the second link stabilised at 9.6467 s

with a slight overshoot of 0.505% and small exerted efforts. The payload produces the same input signal applied to the payload actuator.
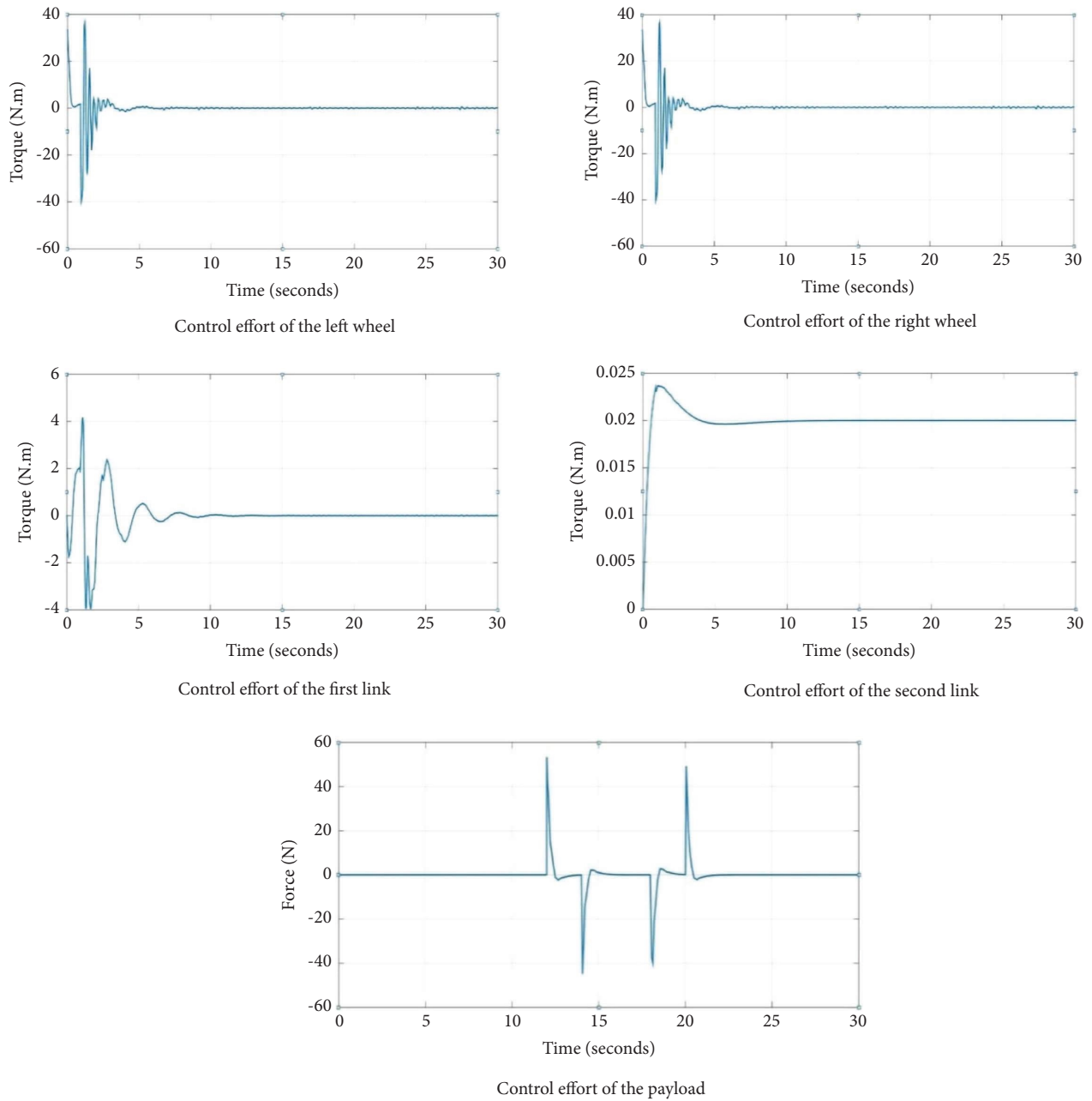
Control effort of the left wheel

Control effort of the right wheel

Control effort of the first link

Control effort of the second link

Control effort of the payload

FIGURE 6: System exerted effort with the first input signal using hybrid controllers.
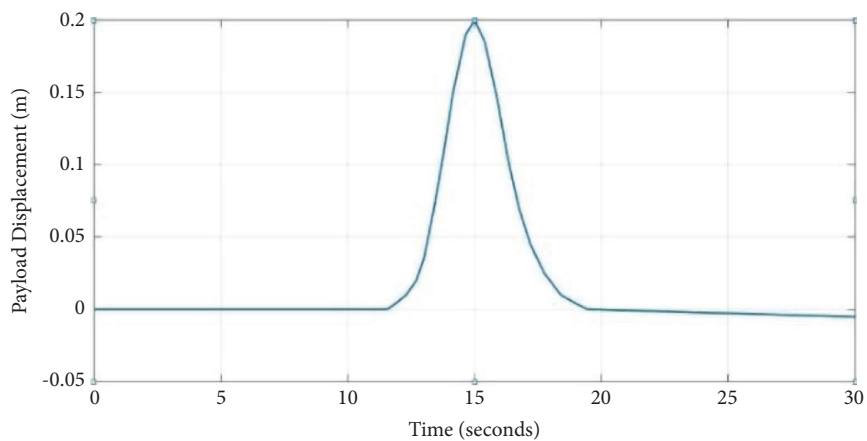
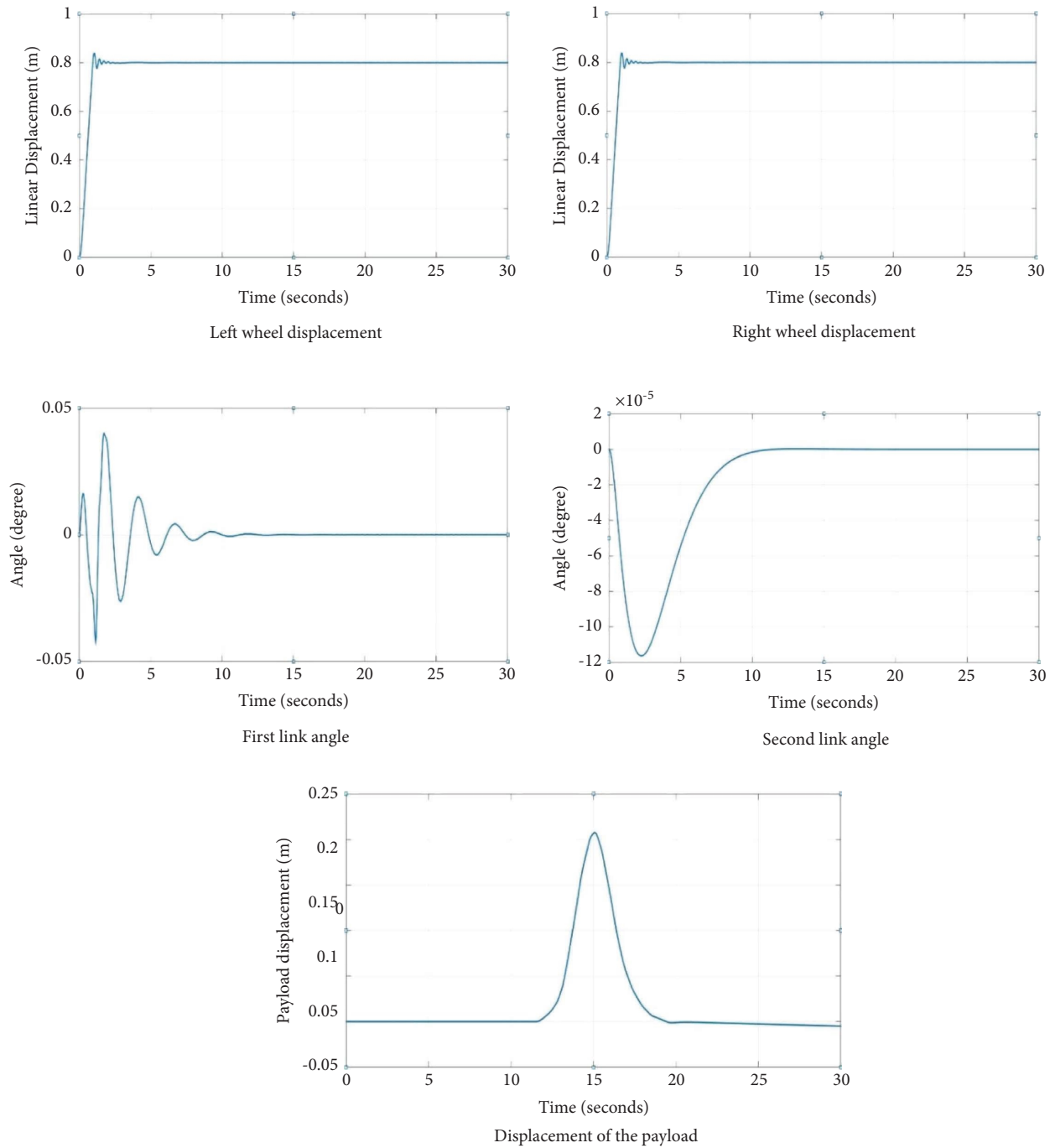FIGURE 7: The second input signal applied on the payload.

Left wheel displacement

Right wheel displacement

First link angle

Second link angle

Displacement of the payload

FIGURE 8: System response with the second input signal using hybrid controllers.

Comparing the simulation results to those reported by [25], the system successfully stabilised with less control effort that provided a stable response, and the wheels stabilised at 36.4 N.m. The first link controller effort was 4.15 N.m, which gave satisfactory responses, while in the previous study, the wheels stabilised with more than 120 N.m further more than 7 N.m controller effort exerted for the first link.
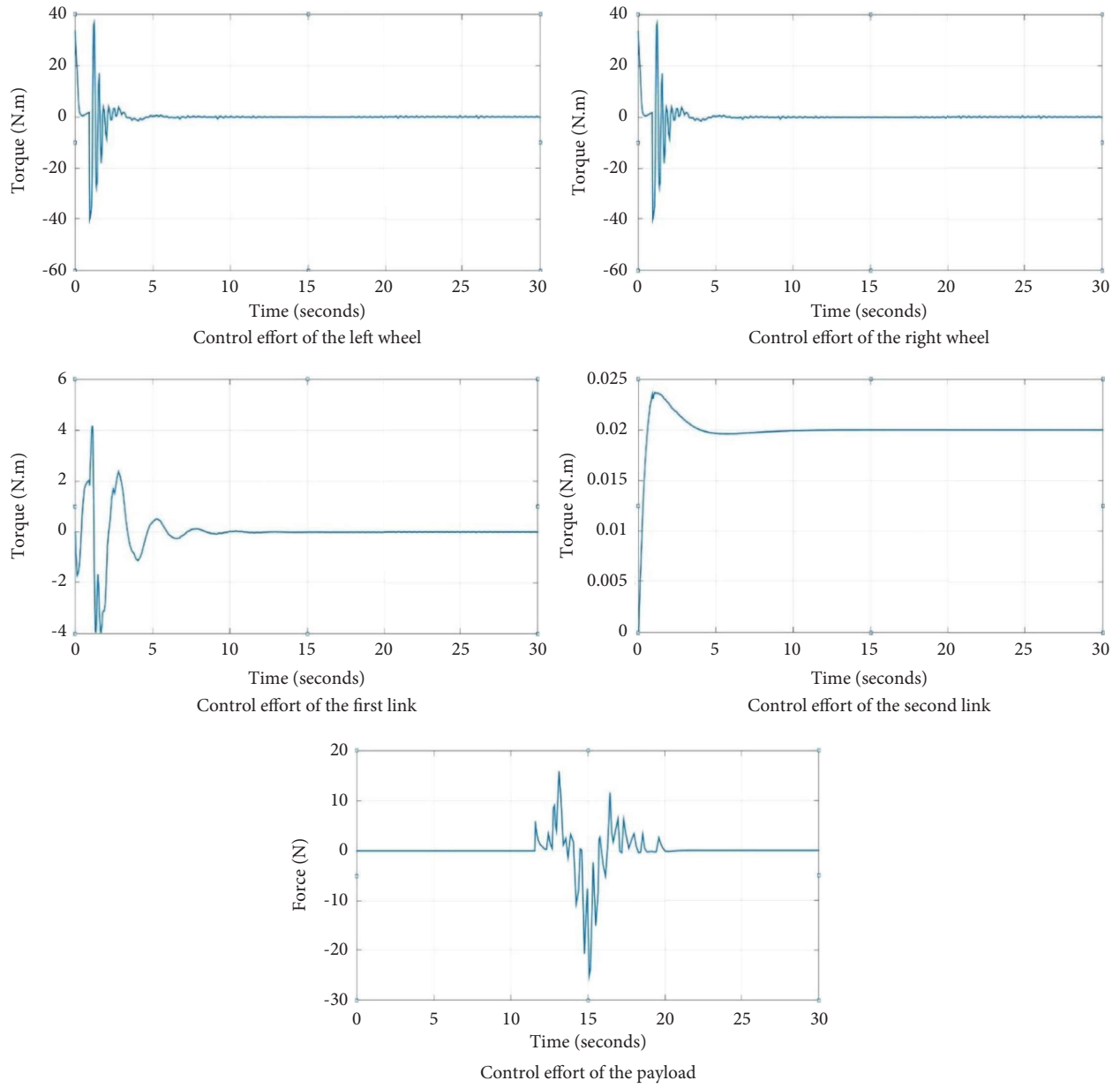
Figure 9: :System exerted effort with the second input signal using hybrid controllers.
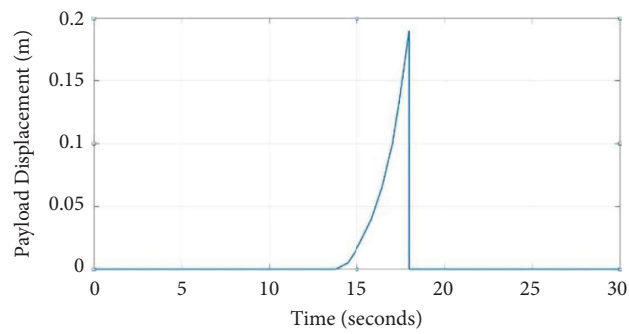

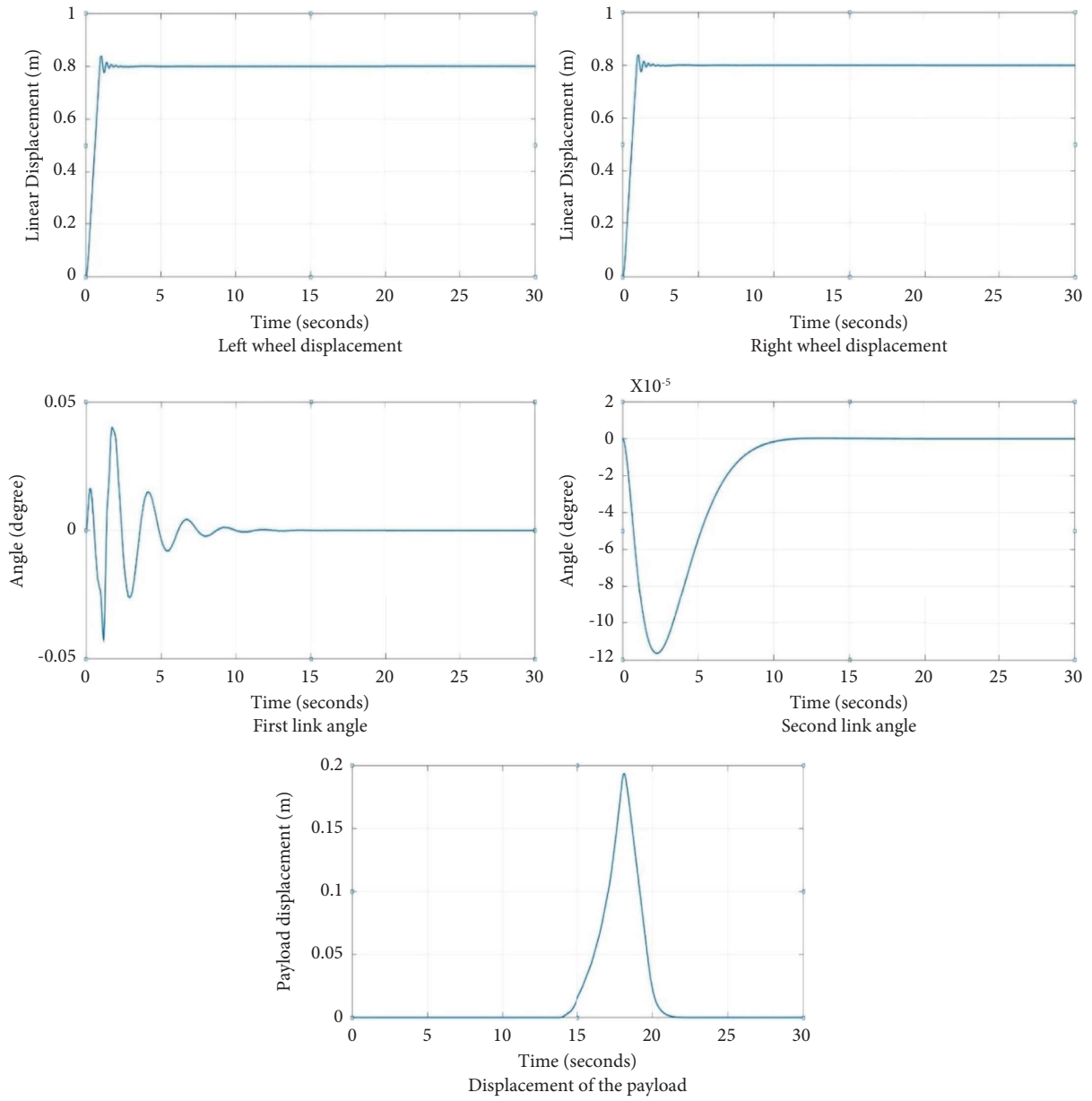Figure 10: The third input signal applied on the payload.

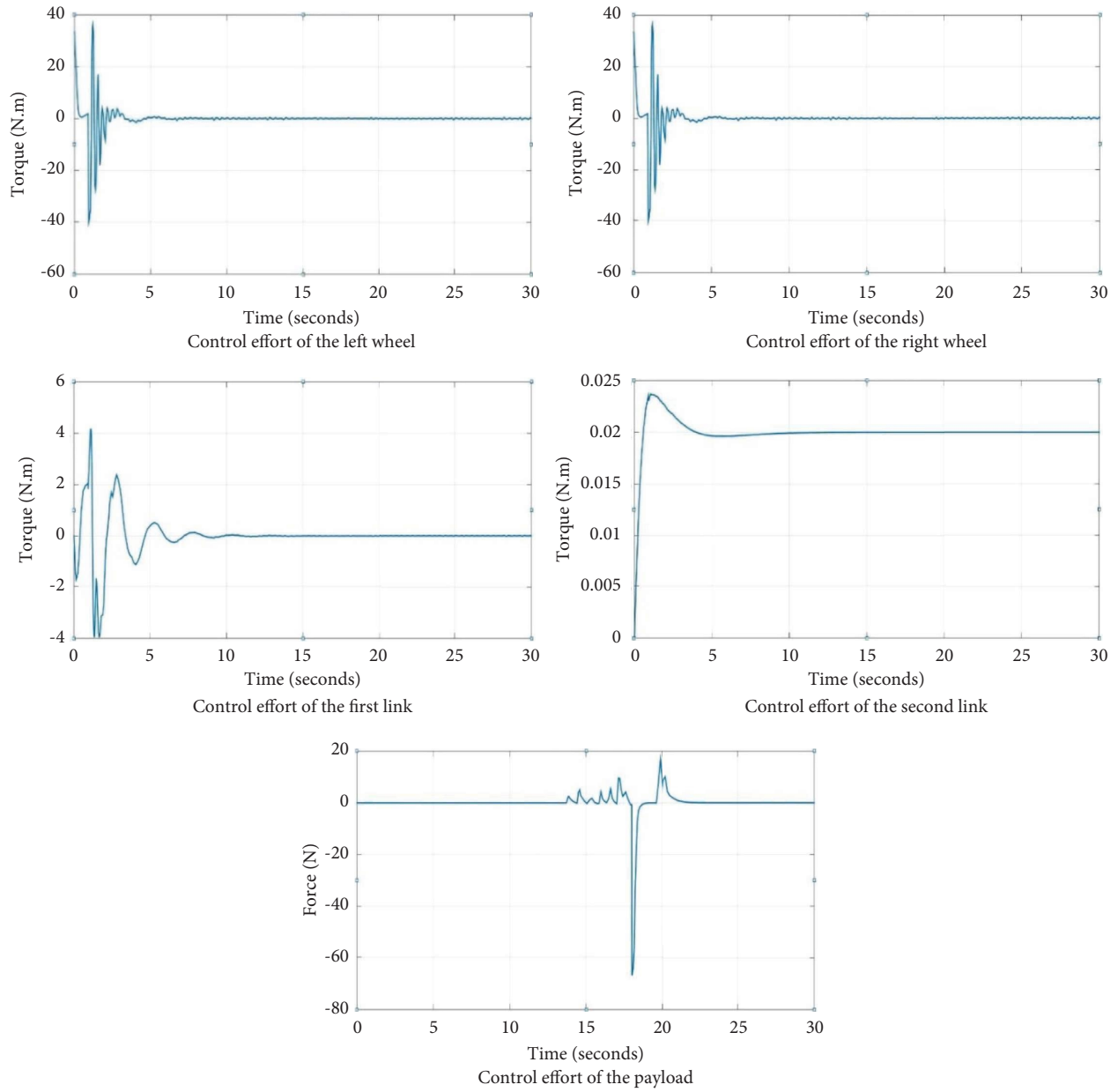FIGURE 11: System response with the third input signal using hybrid controllers.

Figure 12: System exerted effort with the third input signal using hybrid controllers.
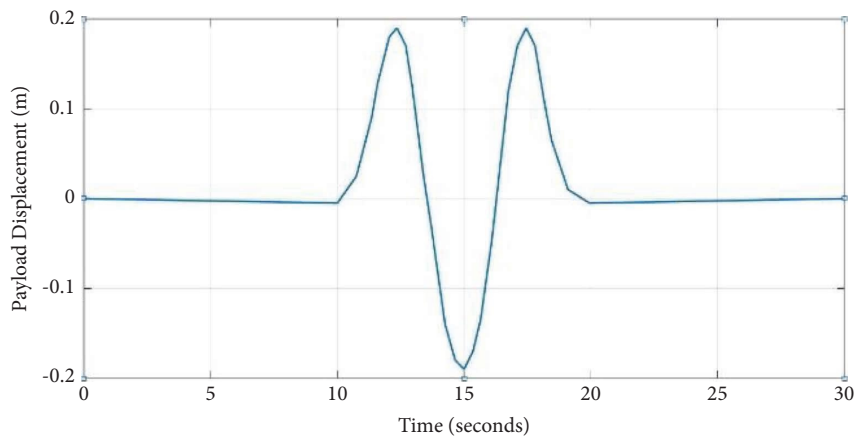

Figure 13: The fourth input signal applied on the payload.

Left wheel displacement

Right wheel displacement

First link angle

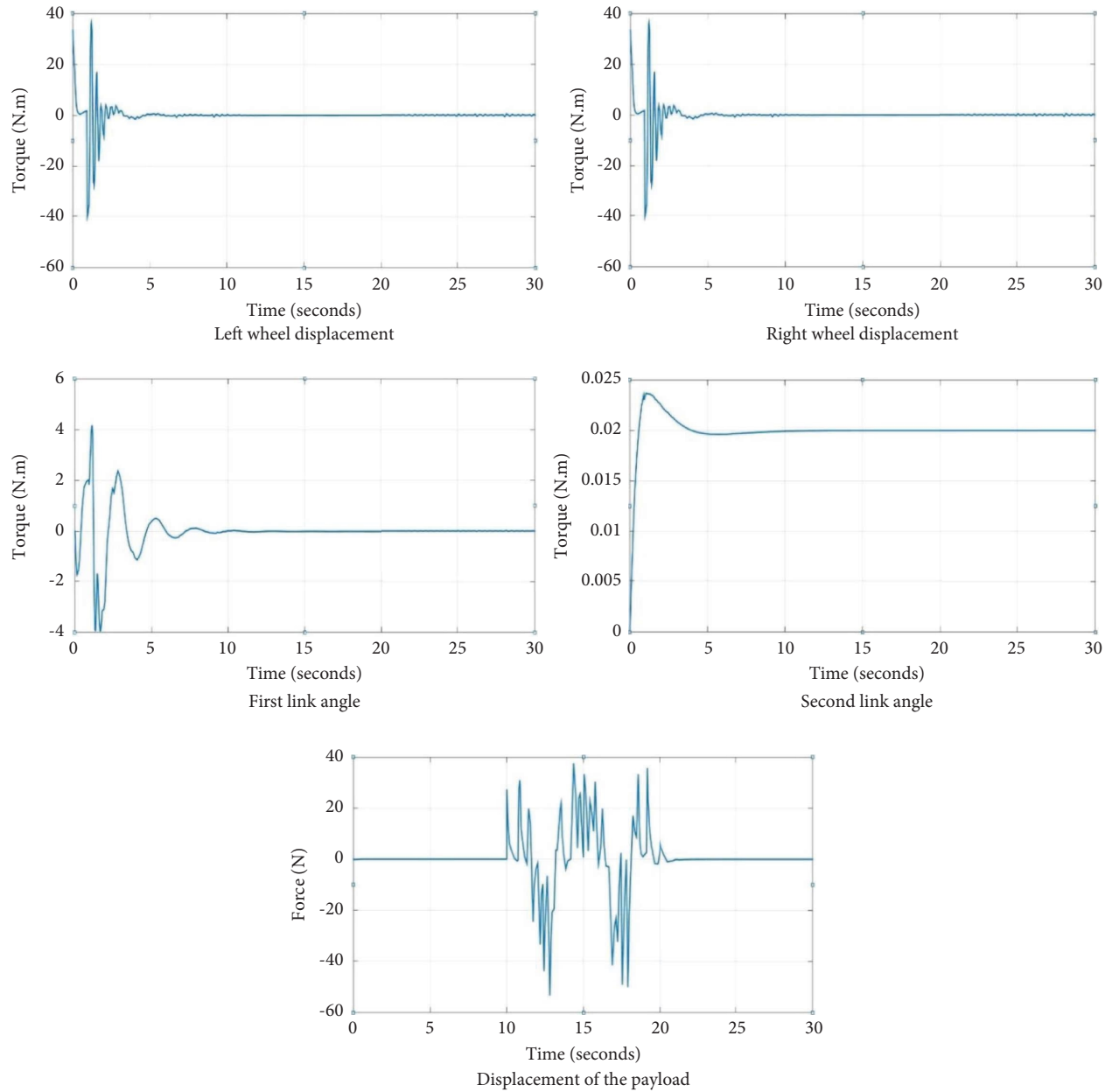Second link angle

Displacement of the payload

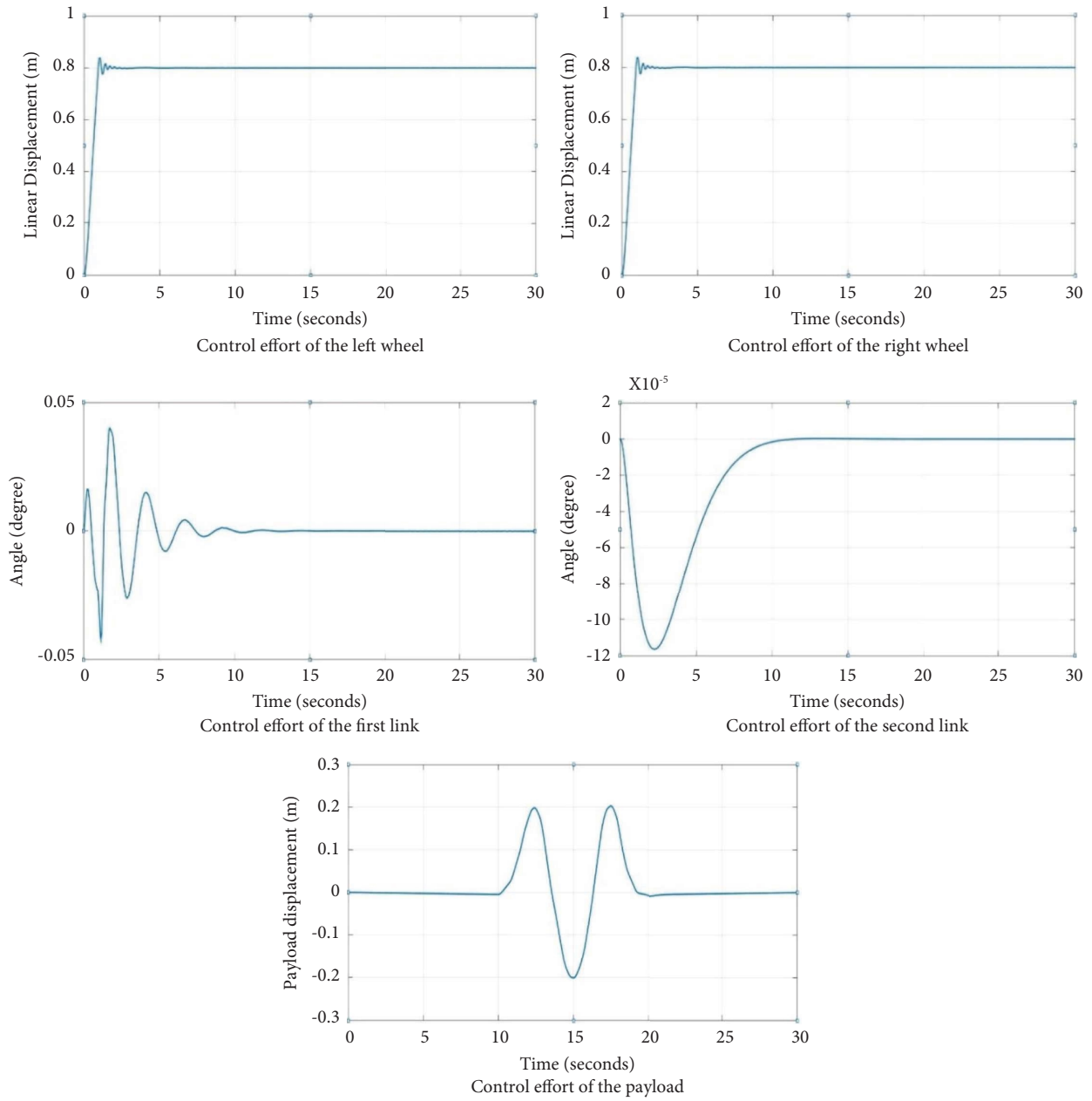Figure 14: System exerted effort with the fourth input signal using hybrid controllers.

Figure 15: System response with the fourth input signal using hybrid controllers.

TABLE 4: The utilised terms and their definitions [35].

Variables and Units	Description
$L_{M(t)}$ (m)	Distance from the centre of mass to the payload
$L_{2u(t)}$ (m)	Distance from the centre of mass to the upper part of 2nd link
L_a (m)	Linear actuator position
L_1 (m)	The half-length of the 1st link
H (m)	The separating two wheels' distance
Q (m)	The displacement of the actuator
M_1 (KG)	The 1st link mass
M_m (Kg)	The motor mass that drives the 2nd link
M_{2l}, M_{2u} (Kg)	The lower-upper parts mass of the 2nd link
M_a (Kg)	Linear actuator mass
M (Kg)	Mass of the payload
M_w (Kg)	Mass of the wheels
T_R, T_L (N · m)	Torques driving left-right wheels
T_m (N · m)	The motor torque
F_a (N)	The linear actuator force
F_f (N)	The linear actuator frictional force
F_d (N)	The external force
θ_1 (rad)	The angle of the 1st link
θ_2 (rad)	The angle of the 2nd link
$\varnothing$ (rad)	The angle measured around the Z-axis
δ_R, δ_L (m)	The angular displacement of both wheels
J_1 (Kg · m^2)	Mass moment of inertia of the 1st link
J_{2u}, J_{2l} (Kg · m^2)	Mass moment of inertia of the 2nd link upper-lower parts
J_a (Kg · m^2)	The actuator's mass moment of inertia
J_M (Kg · m^2)	The payload's mass moment of inertia
J_w (Kg · m^2)	Both wheels' mass moment of inertia
J_{IB} (Kg · m^2)	The intermediate body's mass moment of inertia

5. Conclusion and Future Work

This paper's objective was to design a hybrid control system for a two-wheeled robot vehicle with a movable payload based on the double-inverted pendulum system. The hybrid controller consists of PID with FLC and PD with FLC used for the system stabilisation. The PID and PD controllers were tuned progressively while the FLC was designed with five MFs and a 25-rules base. The simulation results illustrated that the hybrid control system was successfully designed to control the robot vehicle. The validation of the designed controller has been proved by applying different input signals to the payload actuator. The simulation results have shown successful stable responses. Future work should thus focus on testing the control system's robustness by applying disturbances on all system parts with various amplitudes. (see Table 4).

Data Availability

The data used in this study are available from the corresponding author upon reasonable request.

Conflicts of Interest

The authors declare that there are no conflicts of interest in this article.

Acknowledgments

References

[1] K. M. Goher and S. O. Fadlallah, "Bacterial foraging-optimized PID control of a two-wheeled machine with a two-directional handling mechanism," *Robotics and Biomimetics*, vol. 4, p. 1, 2017.

[2] J. Wu and W. Zhang, "Design of fuzzy logic controller for two-wheeled self-balancing robot," in *Proceedings of the 2011 6th International Forum on Strategic Technology IFOST*, vol. 2, pp. 1266–1270, Harbin, China, August 2011.

[3] J. Wu, W. Zhang, and S. Wang, "A two-wheeled self-balancing robot with the fuzzy PD control method," *Mathematical Problems in Engineering*, vol. 2012, Article ID 469491, 13 pages, 2012.

[4] Y. Liu, Z. Chen, D. Xue, and X. Xu, "Real-time controlling of inverted pendulum by fuzzy logic," in *Proceedings of the 2009 IEEE International Conference on Automation and Logistics*, pp. 1180–1183, Shenyang, China, August 2009.

[5] M. Bettayeb, C. Boussalem, R. Mansouri, and U. M. Al-Saggaf, "Stabilization of an inverted pendulum-cart system by fractional PI-state feedback," *ISA Transactions*, vol. 53, no. 2, pp. 508–516, 2014.

[6] S. Hanwate, Y. V. Hote, and A. Budhraja, "Design and implementation of adaptive control logic for cart-inverted pendulum system," *Proceedings of the Institution of Mechanical Engineers—Part I: Journal of Systems & Control Engineering*, vol. 233, no. 2, pp. 164–178, 2019.

[7] A. Gani, Ö. Lu, H. Açikgöz, and Ş. İ. Ekkel, "Fuzzy logic controller design based on sugeno inference method for nonlinear inverted pendulum dynamical systems," *Sigma Journal of Engineering and Natural Sciences*, vol. 8, no. 1, pp. 19–30, 2017.

[8] W. Aribowo, T. Yamashita, and K. Terashima, "Integrated trajectory planning and sloshing suppression for three-dimensional motion of liquid container transfer robot arm," *Journal of Robotics*, vol. 2015, Article ID 279460, 15 pages, 2015.

[9] L. T. Aguilar, "Output feedback nonlinear H ∞ -tracking control of a nonminimum-phase 2-DOF underactuated mechanical system," *Journal of Robotics*, vol. 2009, Article ID 718728, 10 pages, 2009.

[10] T. A. Albhkali, "An impulse-momentum approach to swing-up control of double inverted pendulum on a cart," *World Academy of Science, Engineering and Technology*, vol. 78, pp. 762–768, 2011.

[11] S. K. Yadav and S. Sharma, "Optimal control of double inverted pendulum using LQR controller," *International Journal of Advanced Research in Computer Science and Software Engineering*, vol. 2, no. 2, pp. 189–192, 2012.

[12] E. E. Eldukhri and H. G. Kamil, "Optimisation of swing-up control parameters for a robot gymnast using the bees algorithm," *Journal of Intelligent Manufacturing*, vol. 26, no. 5, pp. 1039–1047, 2015.

[13] H. G. Kamil, A. A. Ahmed, and A. K. Abbas, "Tuning of control motion for a three link robot manipulator using particle swarm optimization technique," *Journal of Kerbala University*, vol. 15, no. 4, pp. 102–110, 2017.

[14] S. Kavirayani and U. Salma, "Fuzzy granular computing controls ill-conditioned matrix definitions for triple inverted pendulum," *Advances in Intelligent Systems and Computing*, Vol. 758, Springer, Singapore, 2018.

[15] M. Jibril, M. Tadese, and E. Tadese, "Comparison of a triple inverted pendulum stabilization using optimal control technique," *International Journal of Electrical and Power Engineering*, vol. 14, no. 6, pp. 60–67, 2020.

[16] A. Fahmi, M. Sulaiman, I. Siradjuddin et al., "Stabilized controller of a two wheels robot," *Bulletin of Electrical Engineering and Informatics*, vol. 9, no. 4, pp. 1357–1363, 2020.

[17] C. Dias, H. Nishiuchi, S. Hyoudo, and T. Todoroki, "Simulating interactions between pedestrians, Segway riders and cyclists in shared spaces using social force model," *Transportation Research Procedia*, vol. 34, pp. 91–98, 2018.

[18] I. K. Mohammed and A. I. Abdulla, "Balancing a Segway robot using LQR controller based on genetic and bacteria foraging optimization algorithms," *TELKOMNIKA (Telecommunication Computing Electronics and Control)*, vol. 18, no. 5, pp. 2642–2653, 2020.

[19] S. Ahmad, N. H. Siddique, and M. O. Tokhi, "A modular fuzzy control approach for two-wheeled wheelchair," *Journal of Intelligent and Robotic Systems*, vol. 64, no. 3-4, pp. 401–426, 2011.

[20] P. N. Dao and Y. C. Liu, "Adaptive reinforcement learning strategy with sliding mode control for unknown and disturbed wheeled inverted pendulum," *International Journal of Control, Automation and Systems*, vol. 19, no. 2, pp. 1139–1150, 2021.

[21] W. Sun, S. F. Su, J. Xia, and Y. Wu, "Adaptive tracking control of wheeled inverted pendulums with periodic disturbances," *IEEE Transactions on Cybernetics*, vol. 50, no. 5, pp. 1867–1876, 2020.

[22] E. Kljuno and R. L. W. Ii, "Humanoid walking robot: modeling, inverse dynamics, and gain scheduling control," *Journal of Robotics*, vol. 2010, Article ID 278597, 19 pages, 2010.

[23] K. Yin, Y. Xue, Y. Yu, and S. Xie, "Variable impedance control for bipedal robot standing balance based on artificial muscle activation model," *Journal of Robotics*, vol. 2021, Article ID 8142161, 9 pages, 2021.

[24] F. Wang, S. Wen, C. Wu, Y. Zhang, and J. Li, "Motion intention analysis-based coordinated control for amputee-prosthesis interaction," *Journal of Robotics*, vol. 2010, Article ID 139634, 1 page, 2010.

[25] A. M. Almeshal, M. O. Tokhi, and K. M. Goher, "Stabilization of a new configurable two-wheeled machine using a PD-PID and a hybrid FL control strategies: a comparative study," in *Proceedings of the 32nd International Conference on Control, Automation and Robotics (ICCAR 2012)*, vol. 6, no. 10, pp. 65–72, Dubai, UAE, October 2012.

[26] V. D. H. Nguyen, X. Huynh, M. Nguyen, I. C. Vladu, and M. Ivanescu, "Hierarchical sliding mode algorithm for athlete robot walking," *Journal of Robotics*, vol. 2017, Article ID 6348980, 13 pages, 2017.

[27] Z. Lijuan and T. Yaqing, "Research of car inverted pendulum model based on Lagrange equation," in *Proceedings of the 2006 6th World Congress on Intelligent Control and Automation*, vol. 1, pp. 820–824, Dalian, China, June 2006.

[28] A. M. Almeshal, K. M. Goher, A. N. K. Nasir, and M. O. Tokhi, "Steering and dynamic performance of a new configuration of a wheelchair on two wheels in various indoor and outdoor environments," in *Proceedings of the 2013 18th International Conference on Methods & Models in Automation & Robotics (MMAR)*, pp. 223–228, Miedzyzdroje, Poland, August 2013.

[29] A. Ziaei, "Inverse dynamics based optimal fuzzy controller for a robot manipulator via particle swarm optimization," *Journal of Robotics*, vol. 2019, Article ID 5052185, 10 pages, 2019.

[30] I. Erenoglu, I. Eksin, E. Yesil, and M. Guzelkaya, "An intelligent hybrid fuzzy PID controller," in *Proceedings of the 20th European Conference on Modelling and Simulation 2006*, vol. 5, pp. 62–66, Bonn, Germany, May 2006.

[31] P. Pratumsuwa, S. Thongchai, and S. Tansriwong, "A hybrid of fuzzy and proportional-integral-derivative controller for electro-hydraulic position servo system," *Energy Research Journal*, vol. 1, no. 2, pp. 62–67, 2010.

[32] J. N. Rai, "Speed control of dc motor using fuzzy logic technique," *IOSR Journal of Electrical and Electronics Engineering*, vol. 3, no. 6, pp. 41–48, 2012.

[33] S. K. Sarkar, F. R. Badal, and S. K. Das, "A comparative study of high performance robust PID controller for grid voltage control of islanded microgrid," *International Journal of Dynamics and Control*, vol. 6, no. 3, pp. 1207–1217, 2018.

[34] K. M. Elbayomy, J. Zongxia, and Z. Huaqing, "PID controller optimization by GA and its performances on the electro-hydraulic servo control system," *Chinese Journal of Aeronautics*, vol. 21, no. 4, pp. 378–384, 2008.

[35] Y. S. Hussein, *Controller Design of Two-Wheeled Robotic Vehicle Based on Fuzzy Logic Technique in Partial Fulfilment of the Requirements for the Degree of Master of Science (MSC) in Electrical Engineering*, University of Kerbala, Karbala, Iraq, 2022.

[36] T. Watanabe and Y. Sugi, "Computer simulation tests of feedback error learning controller with IDM and ISM for functional electrical stimulation in wrist joint control," *Journal of Robotics*, vol. 2010, Article ID 908132, 11 pages, 2010.

[37] A. Aouf, L. Boussaid, and A. Sakly, "Same fuzzy logic controller for two-wheeled mobile robot navigation in strange environments," *Journal of Robotics*, vol. 2019, Article ID 2465219, 11 pages, 2019.

[38] N. T. Vu and N. P. Tran, "Path planning for excavator arm: fuzzy logic control approach," *Journal of Robotics*, vol. 2020, Article ID 8893260, 10 pages, 2020.